The process of frequency doubling in birefringent, non-centrosymetric crystals is one of the most commonly applied nonlinear processes in laser technology. Frequency doubling or second harmonic generation is an energy and impulse conserving process. While the conservation of energy is easily meet by doubling the frequency, the conservation of the impulse is more complicated. This is due to substantial dispersion of the refractive index in an optically dense medium such as a crystal (Fig. 6). This leads to the innate shift in the velocity of light generated at double the frequency with respect to the original fundamental wave. In order to meet the phase-matching conditions in the velocity of the fundamental frequency and its conversion to its second harmonic in a medium, the different values for the refractive index in the ordinary and extraordinary axis of a bifringent crystal are utilized. By placing the optical axis of the crystal at a specific angle to the polarization of the incoming fundamental beam, the effective refractive index for the different frequencies can be compensated according to $n_\nu = n_{2\nu}$. This allows for the conservation of impulse to be realized in matching the phase of the fundamental and second harmonic frequency in their propagation through the crystal. Common materials used for this purpose are BBO (&-barium borate), KTP (potassium titanyl phosphate), LBO (lithium triborat) or LiNbO3 (lithium niobate) crystals.

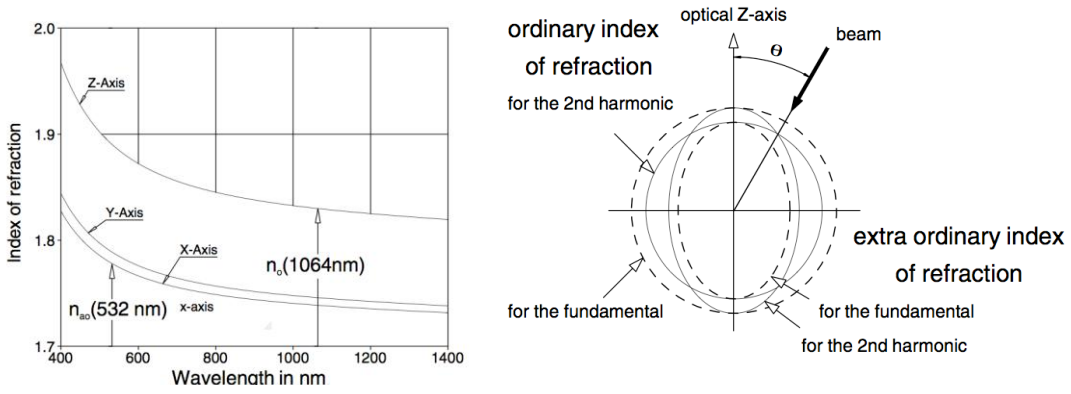

Fig. 6: Dispersion curve for the fundamental and second harmonic of the Nd:YAG laser in KTP (left). Schematic representation of a refractive index ellipsoid for achieving phase-matching in second harmonic generation within a birefringent, nonlinear crystal (right). [6]

3 Experimental setup

3.1 Description of equipments

Fig. 7 shows the outline of the experimental setup. All components were mounted and clamped on a slide rail labeled as module S. Module A is the laser diode, which emits a pump light with a temperature dependent wavelength, followed by the collimator (module B) and the focusing unit (module C). The collimator consists of a three-lens system with a short focal length of 6mm. It collimates the strongly divergent laser diode beam. The

focusing unit has a focal length of 60mm which focuses the collimated diode laser beam into the Nd:YAG rod which itself is mounted in module D. This module D along with module E forms the resonator. On one end of the YAG rod a highly reflective coating is deposited which is used as the left mirror of the resonator. The right resonator mirror is mounted in module E. It has a radius of curvature of R = 100mm and has a high reflectivity for wavelengths of 1064nm. Module E is used as the output coupler.

For second harmonic generation a mirror with highly reflective coating at center wavelength 1064 nm and a high transmission at center wavelength 532nm is used in the output coupler. Module F is the filter plate holder. Two different filters were used. The color filter RG1000 suppresses the pumping radiation of 808 nm. The second filter BG39 allows only the radiation of 532 nm to pass. Module G is the photodiode which was used for the relative measurements of the laser output power. A power meter was also used in certain cases. An adjustable aperture (not shown in the diagram) was used while performing the continuous wave operation and for the second harmonic generation operation this aperture was replaced by a KTP (Potassium titanyl phosphate) crystal which is mounted in module K. For the Q-switched operation a Pockel's cell (module P) was used along with a high voltage supply (module Z). A power meter (module H) and a PC-oscilloscope (not shown) were used for taking measurements. A CMOS chip (placed at the filter plate holder) was used to detect and record the spatial modes of the beam.

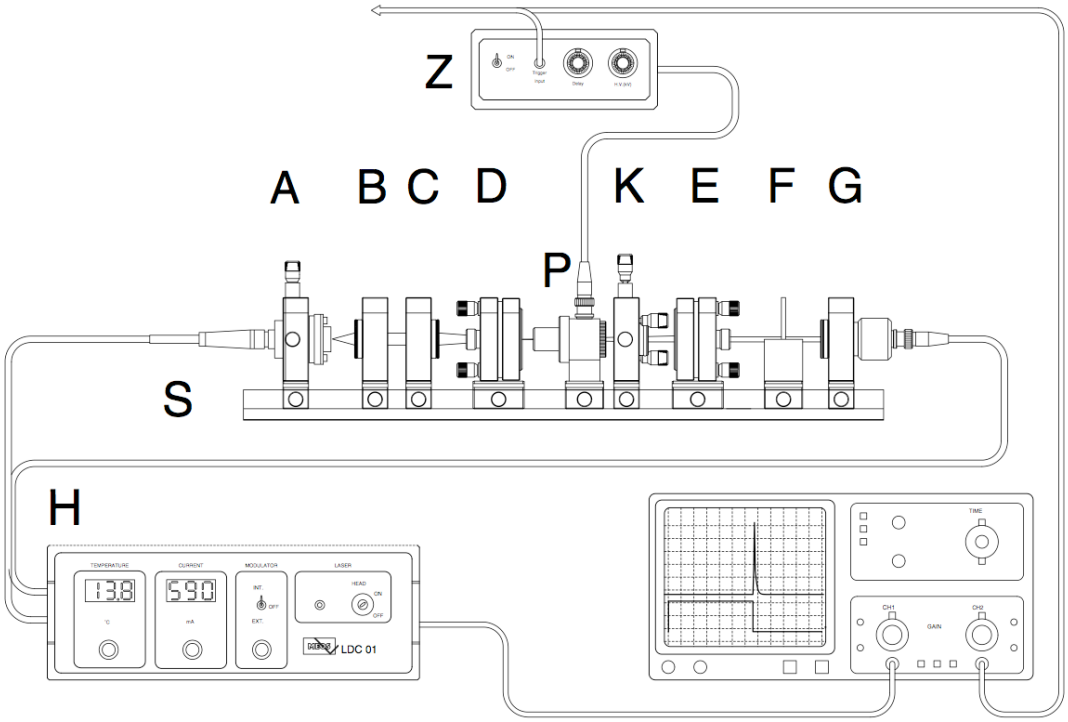

Fig. 7: Experimental setup [7]

3.2 Procedure

The emitted beam at about $\lambda = 808\,nm$ from the diode pump laser was collimated using module A. As mentioned previously, the collimator lens has a focal length of 6 mm. The focus is located about 1-2 mm in front of module A. Thus it was placed as close to the diode laser as possible without touching it. The collimator was then adjusted (using the adjustment screws) such that the beam profile took the form of a flat rectangle (when viewed from side) and hit the photodiode at the centre and was also parallel with the horizontal. Then using module B the beam was focused into the Nd:YAG rod. Since the focal length of this lens is 60 mm, the YAG rod should be positioned at about this distance so that the focus is located within the rod. The output coupler was mounted. The distance between the YAG rod and the output coupler was determined using the stability criterion (eq. 2). Since the mirror on the rod is assumed to be flat, it has the radius of curvature $R \to \infty$, while the output coupler has $R = 100$ mm. Consequently the cavity length L must be $0 \leq L \leq 100$ mm. The rod and the output coupler were aligned parallel to the optical axes and the constructed cavity was adjusted for maximal output. It is to be mentioned here that before placing a component, the diode laser was switched off every time to avoid any possible accidents. The laser output beam was made to be visible with an IR converter screen.

4 Results and analysis

4.1 Continuous wave operation at 1064 nm

The continuous wave operation was performed in order to measure the threshold pump power for lasing and the efficiency of the Nd:YAG laser for resonant pumping of the 808 nm transition in the Nd:YAG medium. The apparatus is setup as described previously. Spatial mode is detected with the CMOS chip using the aperture which limits the angles of the modes. The aperture is adjusted to obtain the TEM_{00} mode with maximum output power. To calibrate the pump current to the pump power, we measured the output power at three current values at fixed wavelength (808 nm) and different temperatures. Applying a linear fit, we got a calibration equation of

$$P_{pump} = I_d \cdot (0.00106)\frac{mW}{mA} - 0.167mW. \qquad \text{(Eq. 6)}$$

The photo diode was used to record the voltage values of the output laser at different diode current values at 33°C. At high power levels the photodiode saturates, hence neutral density filters (optical density d=3) were used to suppress the output power so that it is within the range of the photo diode. To calibrate the photodiode, we measured the laser output power without filters at three currents and the corresponding voltage values at the same currents, this time with the neutral filters applied. Applying a linear fit, we got the calibration equation:

$$P_{output} = U_d \cdot (0.0334)\frac{mW}{mV} + 0.0649mW. \qquad \text{(Eq. 7)}$$

Using these equations, we calculated the pump and laser output power from the current and voltage values and plotted them in Fig. 8. Note: The wavelength of the pump light at constant temperature changes with the applied current. Since the Nd:YAG crystal changes its absorption rate with the wavelength of the incident light, the output power will be different at different wavelengths as well. We neglected this fact in the calibration above. To estimate the amplitude of the error that was made, we measured the voltage at a constant current over a temperature range of 28-36°C, resulting in a deviation about 3%.

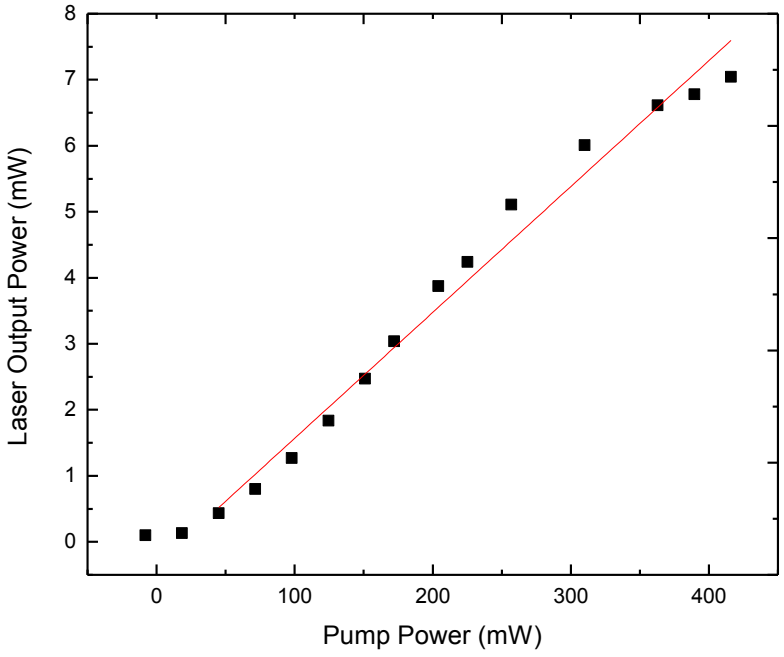

. Fig. 8: Plot of laser output power against diode laser pump power for a continuous wave operation at 1064 nm.

From this plot the threshold pump power is observed to at $P_{threshold} = 45$ mW, while the slope efficiency is easily found from the slope, $\eta = 0.01907$. Furthermore, the intracavity power is calculated using $P_{intra} = [(1 + R)/(1 - R)] \cdot P_{out}$, where P_{out} is the laser output power and R is the reflectivity of the output coupler which is assumed to be as 0.98. The different intacavity power values are tabulated below along with the respective current, pump power and output power values.

Current (mA)	Pump power (mW)	Voltage (mV)	Output power (mW)	Intracavity power (mW)
175	18.5	2	0.1317	13.0
200	45	11	0.4323	42.8
225	71.5	22	0.7997	79.2
250	98	36	1.2673	125.5
275	124.5	53	1.8351	181.7
300	151	72	2.4697	244.5
320	172.2	89	3.0375	300.7
350	204	114	3.8725	383.4
370	225.2	125	4.2399	419.8
400	257	151	5.1083	505.7
450	310	178	6.0101	595.0
500	363	196	6.6113	654.5
525	289.5	201	6.7783	671.1
550	416	209	7.0455	697.5

Table 1: Summary of measurements for the continuous wave operation at 1064 nm.

Next, different transversal modes of the Nd:YAG were tried to be identified. The CMOS chip was used to detect the output of the laser. By changing the angles of the output coupler different transversal modes were obtained and the images of the modes were recorded. Initially this was performed without the aperture. Later however, it was used since the modes could not be defined clearly. The recorded 8-bit gray scale images then were

converted into 2-dimensional numeric arrays by taking the cross-section along a symmetry line which is shown in the figures below. These arrays were then used to identify the different transversal modes and to produce a fit using the Hermite-Gaussian polynomials. Since the cross-section was taken along a symmetry line, the polynomials are reduced to the form

$$I_m(x,0) = I_0\left[H_m\left(\frac{\sqrt{2}(x-xc)}{w}\right)exp\left(-\frac{(x-xc)^2}{w^2}\right)\right], \qquad \text{(Eq. 8)}$$

where m is the order of the rectangular TEM_{m0} mode, w the Gaussian beam radius and H_m the m^{th} Hermite-polynomial. From the number of maxima, we deduced that we observed the TEM_{00}, TEM_{10} and TEM_{50} modes and computed the fit with originlab. The results are shown in Fig. 9, 10 and 11. The particular poor fit of the TEM_{50} mode is likely to be caused by the fact that significant parts of the ends of the mode were cut off.

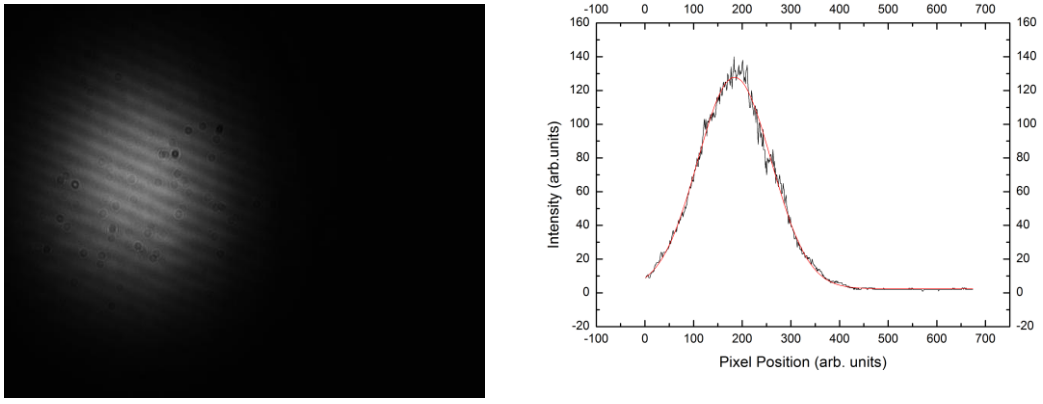

Fig. 9: TEM_{00} mode (Gaussian profile)

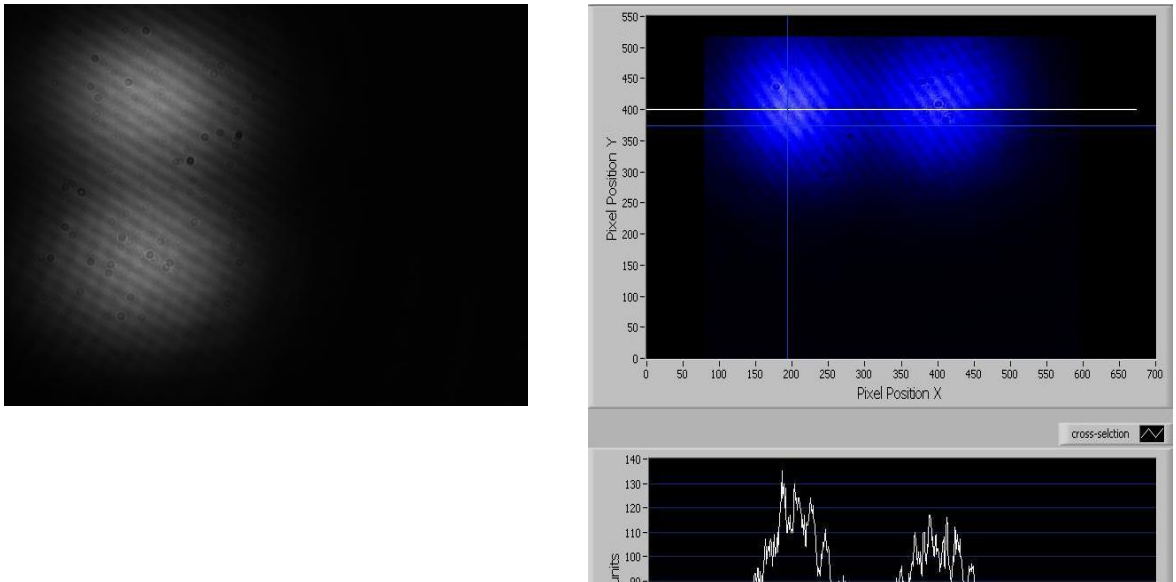

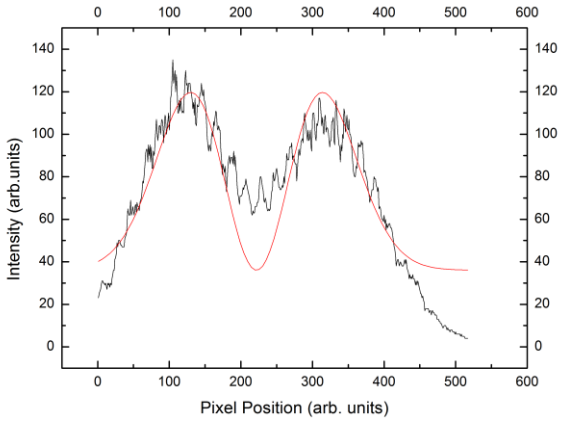

Fig. 10: TEM_{10} mode (Hermite-Gaussian profile)

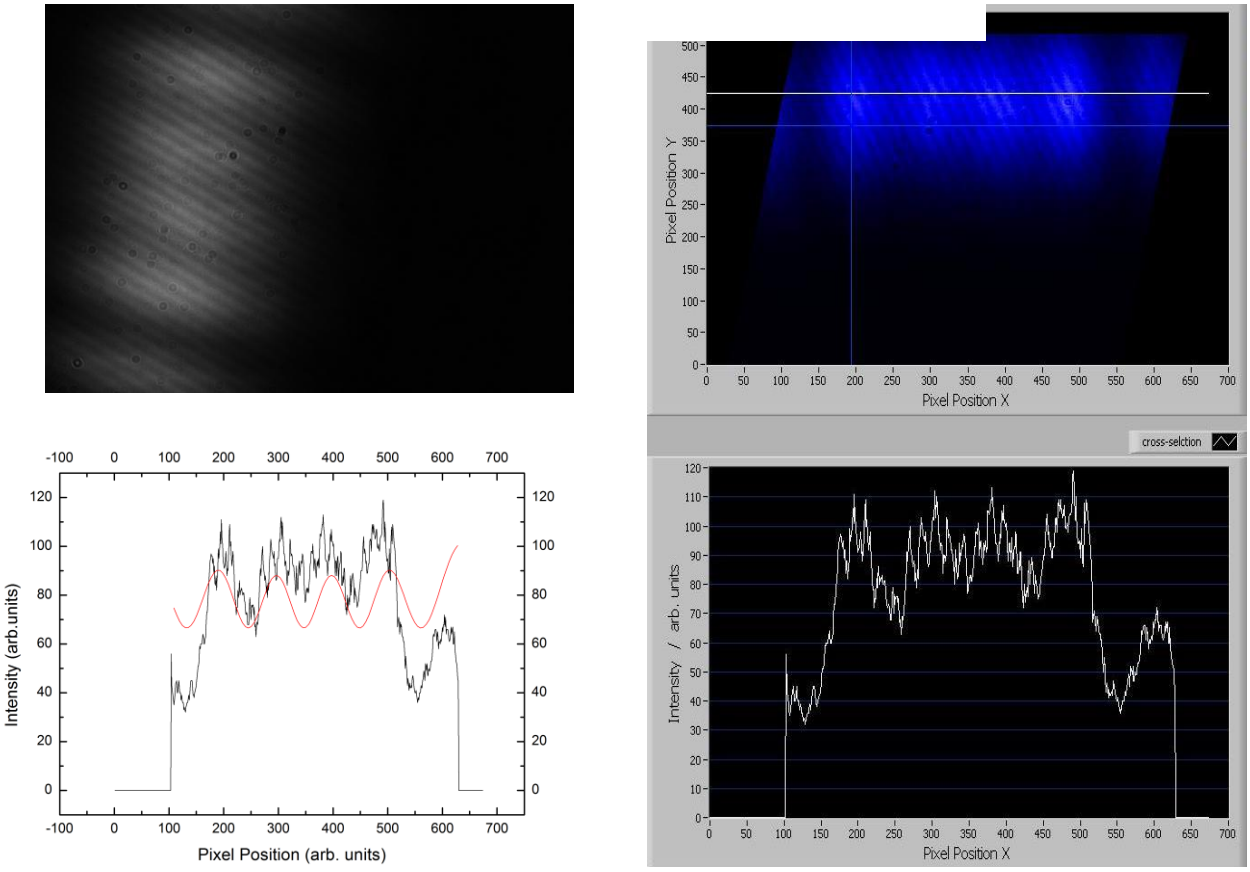

Fig. 11: TEM_{50} mode (Hermite-Gaussian profile)

4.2 Second harmonic generation

To operate a continous wave in the intracavity second harmonic generation the KTP crystal, contained in module K, was placed into the cavity and clamped on the rail. The

mirror in the output coupler was changes as mentioned before. This time the aperture was not used. The module was adjusted so that the crystal was aligned producing maximum output power at 532 nm. The output power was measured using a power meter and the values with their respective pump power and pump current are tabulated below in Table 2. The intracavity efficiency $\eta_{intra} = P_{intra}/P_{pump}$ was calculated using the intracavity power values from part a) as an approximation. The error made here can be assumed to be small, since the losses of the refractor are in the range of 2%. A plot of laser output power against diode laser pump power is shown in Fig. 12. As expected, the output power shows a quadratic relationship (§ 2.7).

Pump current (mA)	Pump power (mW)	Laser output power (mW)	Efficiency	Intracavity efficiency
175	18.08	0.7	0.03872	0.719
200	44.58	0.09	0.0016	0.960
200	44.58	0.1	0.0016	0.960
224	70.02	0.12	0.00258	1.131
250	97.58	0.2	0.00363	1.286
275	124.08	0.29	0.00465	1.464
300	150.58	0.45	0.00566	1.624
325	177.08	0.59	0.00668	1.703
350	203.58	0.86	0.00769	1.883
350	203.58	0.76	0.00769	1.883
375	230.08	1.05	0.0087	1.746
400	256.58	1.34	0.00972	1.971
425	283.08	1.57	0.01073	1.772
450	309.58	1.81	0.01175	1.922
475	336.08	2.2	0.01276	1.791
500	362.58	2.36	0.01378	1.805
525	389.08	2.85	0.01479	1.725
525	389.08	3.15	0.01479	1.725
550	415.58	3.03	0.01581	1.678
550	415.58	3.49	0.01581	1.678

Table 2: Summary of measurements for a continuous wave operation at intracavity second harmonic mode

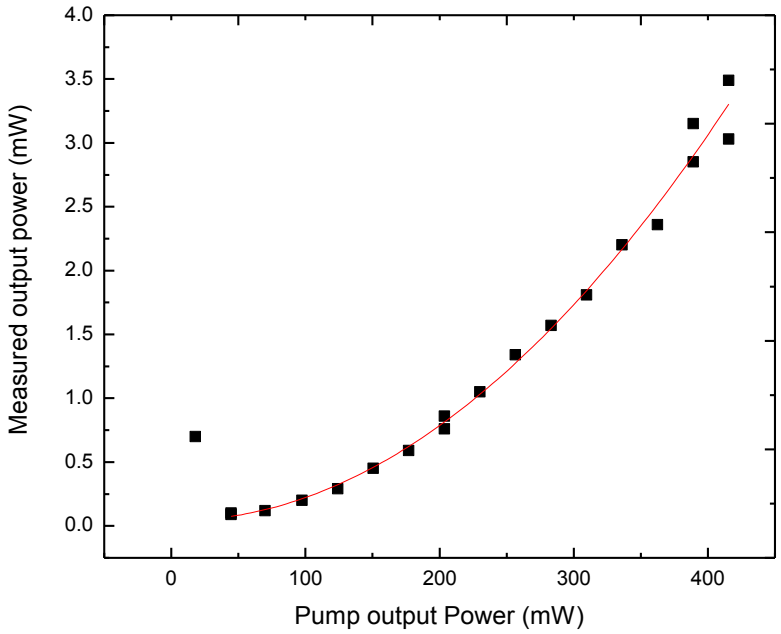

Fig. 12: Plot of laser output power against diode laser pump power for a continuous wave operation at intracavity second harmonic mode.

We applied a 2nd order polynomial fit; its first derivative gives the efficiency as a function of the pump power which is: $\eta_{2nd} = (1.91433 \cdot 10^{-5})P_{pump} - (1.04189 \cdot 10^{-4})$.

In addition, aligned the output coupler very close to the KTP crystal and tried to adjust the mirror to maximum output power. All attempts were unsuccessful, since in this setup the concentration of the light in the crystal is very low and due to the quadratic dependence of the frequency conversion on the intensity of the incoming light, no significant output can be expected.

4.3 Pulsed operation

A pulsed laser output was obtained by operating the Nd:YAG laser in a Q-switched mode with intracivity second harmonic generation. For this purpose a Pockels cell was inserted into the cavity with its voltage supply turned off. A leakage from the cavity was observed at 90° to the original propagation. This happens because as the linearly polarized incident beam (inside the cavity) passes the Pockels cell, it is circularly polarized. Then, after reflection from the rare cavity mirror, when the beam passes the cell a second time, it is again linearly polarized but this time the plane of polarization is rotated by 90°.

The components were adjusted so that the leakage was at maximum for a maximum pump power (571mA). Also the output power was maximized with the Pockels cell voltage supply now turned on. The frequency generator was then turned on which triggered the voltage supply at a frequency of 1000Hz. Using the photodiode without the neutral filters, the pulse trains were observed on the PC-oscilloscope. The frequency generator was adjusted to obtain an observable pulse on the oscilloscope (Fig. 13).

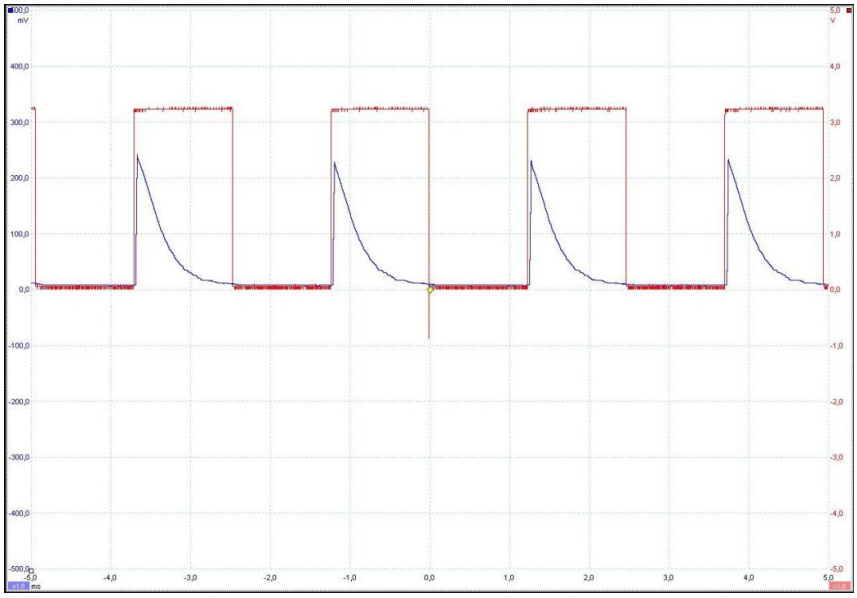

Fig. 13: PC-oscilloscope image. The emitted pulse is colored blue and the trigger pulse is colored red.

From the oscilloscope image, we got a approximate rise time of $t_r = 0.02$ ms and fall time of $t_f = 0.67$ ms (from 10% to 90% and vice versa), repetition rate of 1/2.47ms=0.4 kHz (from peak to peak) and FWHM = 0.03 ms. The shape of the curve should be Gaussian and therefore show equal rise and fall times, thus we conclude that the oscilloscope distorts the pulse shape.

The power of the pulse was below the sensitivity of the power meter, thus we used voltage calibration of the photodiode from part a) to estimate the pulse power. From the pc-oscilloscope, we estimate a pulse peak voltage of about 230mV and time-average voltage of 343 mV/ms. Including the absence of the filters in the calibration equation, this corresponds to a pulse peak power of 7.75 μW and 11.52 μW /ms, respectively. The large power losses can be explained due to losses at the Brewster window at the end of the Pockels cell and losses in the cell itself.

5 References

[1] W. T. Silfvast, *Laser Fundamentals*, 2nd Edition, Cambridge University Press, Cambridge, 2004.

[2] Eichler, Jürgen; Eichler, Hans J.; *Laser*; 3rd Edition; Springer-Verlag Berlin Heidelberg New York; 1998

[3] E. Hecht, *Optics*, 4th Edition, Addison Wesley, San Francisco, 2002.

[4] Ma 14 - Solid State Laser Principles; Instructions for the Advanced Laboratory Course at Freie Universität Berlin; 2011

[5] Koechner, Walter; *Solid State Laser Engineering*; Springer Series in Optical Sciences; 6th Edition; Springer Science+Business Media, Inc.; 2006

[6] R. W. Boyd, *Nonlinear Optics*, 2nd Edition, Academic Press, San Diego, 1995.

[7] K. Dickmann, *Diode laser pumped Nd:YAG Laser*, (operation manual to the Nd:YAG Laser and advanced laboratory experiments), MEOS Cooperation.